

Article citation info:

Sioma A., Lenty B. 2025. Imaging Fungal Infections on Wood Surfaces Based on a Vision System. *Drewno. Prace naukowe. Doniesienia. Komunikaty* 68 (215): 00044. <https://doi.org/10.53502/wood-196695>



Łukasiewicz
Puzhan
Institute of
Technology

Drewno. Prace naukowe. Doniesienia. Komunikaty Wood. Research papers. Reports. Announcements

Journal website: <https://drewno-wood.pl>



Imaging Fungal Infections on Wood Surfaces Based on a Vision System

Andrzej Sioma* 

Bartosz Lenty 

AGH University of Krakow, Krakow, Poland

Article info

Received: 21 November 2023

Accepted: 2 December 2024

Published: 25 February 2025

Keywords

vision system
fungal infections of wood
surface imaging
image analysis

This article discusses a method of imaging fungal infections on the surface of wood using a dedicated vision system. Fungal infections develop on the surface of wood during transport and storage. In the production process, qualitative sorting of wood is carried out based on the presence of infections on surfaces. Some infections are clearly visible, e.g. in the form of black blemishes. However, many infections are poorly visible or invisible to operators sorting the material. The vision system discussed here enables the imaging of defects occurring on wood that are invisible to the human eye. Examples of wood surface infections are presented. The developed concept of surface imaging using spectral illumination and a two-camera system is discussed. For the proposed system, the image sensors of the cameras and spectral characteristics of the illuminators are presented. Then, the configuration of the vision system is indicated, and the imaging resolutions for the selected example are determined. Examples of infection images recorded with the use of UV and RGB illuminators are presented. Image analysis was performed using the intensity characteristics method for sample chosen images. The possibility of identifying infected areas using the intensity characteristics of the UV image and the RGB image was evaluated. The imaging results for selected ranges of electromagnetic radiation and selected infections recorded on the surface of wood are discussed. The possibility of observing and identifying infected areas invisible to the human eye was confirmed.

DOI: 10.53502/wood-196695

This is an open access article under the CC BY 4.0 license:

<https://creativecommons.org/licenses/by/4.0/deed.en>.

Introduction

Various types of defects affect the wood supplied from sawmills to plants. Some of them can be described as natural defects occurring in wood, e.g. knots, resin pores and other types of disturbances in the wood structure. The second group consists of defects resulting from how wood is processed, e.g. the presence of bark, wade or cracks. This paper proposes an imaging method for defects present on the wood surface resulting from the development of fungal infections. This is a group of surface defects that develop during the transport or storage of wood.

Inspection of these types of defects is not currently carried out in automated production systems. However, this should be taken into account considering the increase in the level and scope of production automation, related to the extension of the functionality of control systems used to verify the quality parameters of materials used in production. An increase in production efficiency is also associated with an increase in the speed of material transport and a reduction in the cycle time of technological, control and measurement operations.

Standard solutions such as statistical process control (SPC) are often insufficient. In the era of increasing industry automation, it is required to control the

* Corresponding author: sioma@agh.edu.pl

quality of all products leaving the production line (Lenty & Kwiek, 2021; Sioma, 2019b). Manufacturers of technological machines are introducing cyber-physical systems as standard equipment that perform control or measurement tasks during technological operation (Kamiński, 2018).

Methods of wood quality control have been developed for many years, enabling the evaluation of internal parameters of wood and the assessment of dimensions and defects visible on the surface of the wood. Authors propose imaging methods based on ionising radiation, microwaves, and ultrasound to assess internal parameters (Bucur, 2003; Ondrejka et al., 2021). Thermal imaging (Meinlschmidt, 2005) and computed tomography methods (Wei et al., 2009) allow the segmentation of knots, bark, sapwood and heartwood. Wood defects visible on the wood's surface are imaged using monochrome and colour sensors, enabling the construction of a 2D image. These systems detect healthy and damaged knots, cracks or other surface defects (C. Hu et al., 2004a). Most methods of detecting surface defects are based on classical image analysis methods, i.e. image segmentation and area analysis (Funck et al., 2003; Lenty, 2020). Texture analysis methods are successfully used in various fields to detect even small surface inhomogeneities (Romano et al., 2023). However, different types of wood exhibit variability in terms of surface colour and defect shape, which require dedicated image analysis algorithms to control tasks (Du et al., 2021; Lin et al., 2015; Wakaf & Jalab, 2018).

To some extent, a solution to this challenge is the application of artificial intelligence and deep learning methods to analyse defects present on the surface of wood (Haciefendioglu et al., 2022; He et al., 2020). These solutions do not require parametric defect description and are based on images of wood defects used in the training process (J. Hu et al., 2022b). The main limitation on their use in industrial applications is their effectiveness, reported in the literature at 80–90%.

Three-dimensional imaging methods are also used to assess the quality of wood (Sioma, 2015, 2019a). Analysis of a three-dimensional image allows the assessment of defects on the surface of the wood regardless of its colour and texture. The 3D image enables the implementation of measurement tasks and the evaluation of the geometrical structure of the wood, e.g. the presence of bark, wades and machining defects (Sioma, 2020; Sioma et al., 2018). The laser triangulation method may also properly detect fungus visible on the wood surface. It is possible to inspect areas infected with blue stain fungi, visible as bluish-black discoloration on the surface of wood under industrial conditions (Cinal et al., 2023).

Wood supplied from sawmills can be infected with various species of fungi, which arise and develop both at the stage of storage of wood in the forest and during the processing and storage of the material in sawmills at high temperatures and humidity. Literature studies indicate the possibility of growth of three types of fungi, i.e. blue stain fungi, rotten fungi and mould fungi (Jankowiak, 2013; Kubicek et al., 2019; Linnakoski et al., 2010). All of these can coincide on one surface. In the case of developed and evident infections, it is possible to use 2D imaging in the visible light range or 3D imaging to detect and localise infections (Figure 1). However, it has been noted that in the initial development phase, some infections are visible neither by the human eye (Figure 1) nor by imaging in the visible light range. This paper proposes constructing a specialised vision system that enables the observation of infections on wood surfaces in their development phase.

A review of the available literature indicates a research gap in relation to the use of the UV spectral range for fungal detection on wood surfaces. Kammerbauer et al. (2024) proposed an algorithm for detecting wood rot on the log surface using machine learning. The analysed datasets consist of RGB images of a log cross-section, and a 5MPx resolution camera

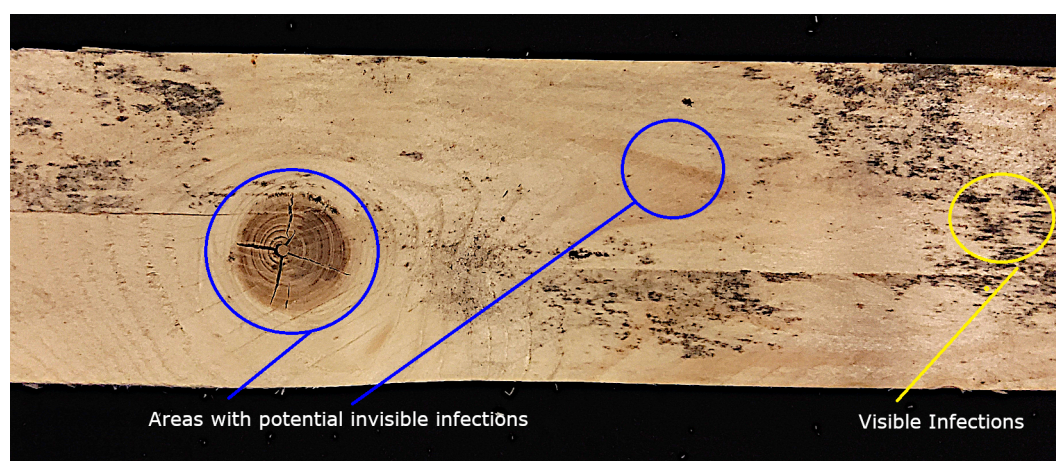


Fig. 1. Wood surface with visible infections (yellow area) and areas where invisible infections may occur (blue area)

and sunlight are utilised. The performance achieved by the proposed model *InternImage-H-UpperNet* is 79%. Another study (Chun et al., 2023) describes approaches to the problem of automatic detection of wood defects, combining classical image analysis methods in the form of edge and blob processing with machine learning and deep learning solutions. A further paper (Yi et al., 2024) deals with wood surface inspection using AI, discussing 12 models and the results achieved by systems employing them. Wells (2018) highlights the difficulty of detecting biological defects in wood by RGB imaging, due to the slight colour differences between infected and healthy areas. X-ray imaging is also rejected due to the limited differences in density at the early stages of infection.

In contrast to the approaches mentioned above, in this work, we propose to enhance the visibility of the defect on the image using UV illumination that triggers photoluminescence in the visible range. We also propose extending the wooden surface imaging capability to 300–1100 nm under RGB+UV illumination. For the designed system, initial design assumptions were made regarding the imaging method, imaging time and imaging resolution. It was also assumed that the system would operate in industrial conditions. Adopting preliminary parameter limits is necessary for selecting the vision system components, including sensors, industrial illuminators and a computer responsible for image analysis. In this case, selecting the type of sensor performing the image acquisition is crucial in preparing the measurement system. It has been shown that choosing an appropriate configuration of sensor and lighting enables the recording of an image of infections invisible to the human eye. It has also been shown that combining imaging in different spectral ranges can expand the range of identified infections on wood. The solution has

been designed for industrial use. Analysing the recorded images enables the identification of various types of infections. The proposed imaging solution could be used to build an industrial-quality control system to detect defects occurring on the surface of wood.

Materials and methods

Manual inspection of wood surfaces in production conditions is carried out using ambient light. In this case, the operators performing this task use a spectrum of electromagnetic radiation in the range 380–780 nm. In order to expand the possibilities of imaging and identifying infections on the wood surface, two cameras and two types of lighting are proposed (Figure 2). The first of the illuminators generates electromagnetic radiation of a wavelength of 385 nm. The second illuminator generates illumination in the visible range by means of RGB LED technology.

The choice of illuminators was based on the assumptions adopted concerning the method of illuminating the surface of the wood and the technical parameters of the illuminator:

- it was decided to use an illuminator with LED technology due to the ability to control the power of the illuminator and the possibility of pulse triggering,
- it was decided to limit the spectral range of UV light to the UV-A range due to the hazardous effect of light in the UV-B and UV-C ranges, which can be dangerous for operators working in production,
- availability of illuminators – the proposed solution was designed with a focus on its future commercialisation. Therefore, the search was restricted to market-available light sources and illuminators designed for industrial use.

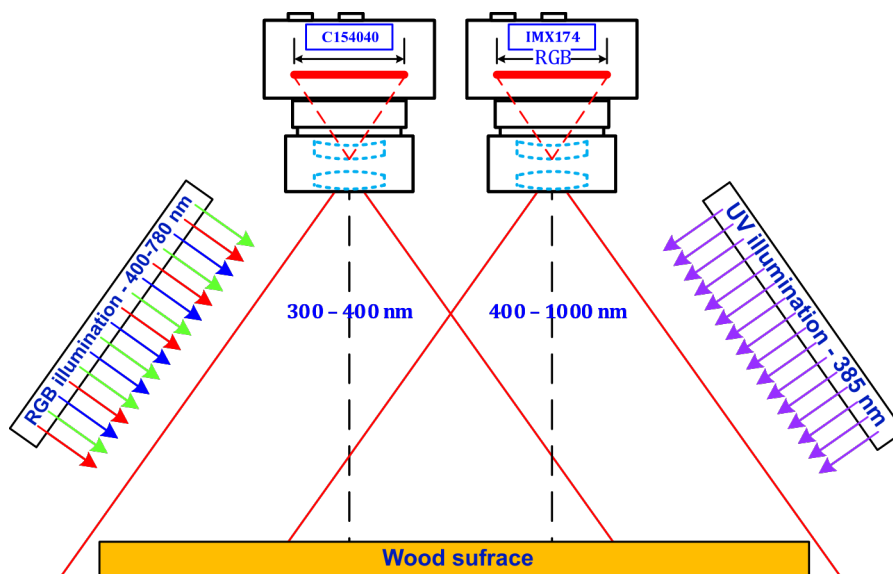


Fig. 2. Imaging stand set-up

An analysis of available solutions on the market indicated the possibility of using UV diodes emitting wavelengths of 365 nm, 385 nm, and 395 nm. In the next step, a comparative experimental study was carried out to determine the influence of the wavelength and the power on the enhancement effect of the defect on the image. The objective was to stimulate the photoluminescence of fungal infections. The comparative study identified an LED with

an average emitted wavelength of 385 nm as the best source for activating photoluminescence. This illuminator allows the emission of light in a bandwidth of approximately 30 nm (Fig. 5). This enables the activation of photoluminescence in several fungal species visible in the recorded images (Fig. 9) with the highest intensity.

An ORCA Fusion BT C154040 camera equipped with a monochrome scientific CMOS sensor with

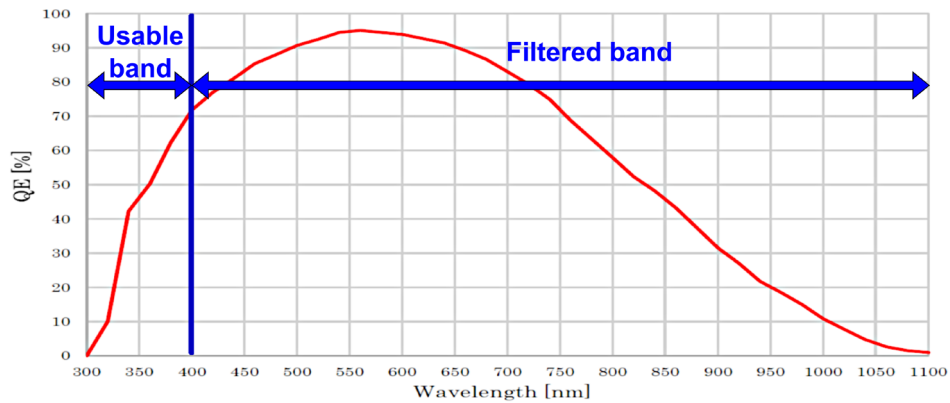


Fig. 3. Quantum efficiency plot of the ORCA Fusion BT C154040 camera

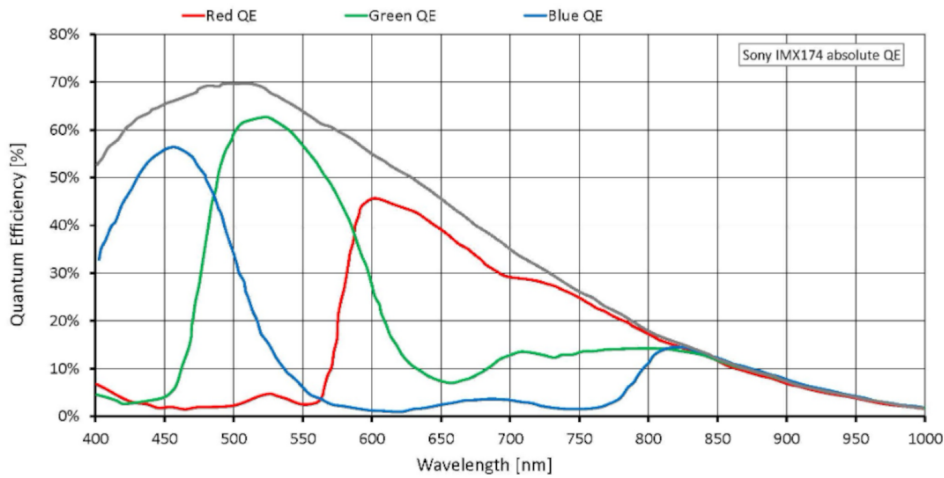


Fig. 4. Quantum efficiency plots of the Sony IMX 174 sensor

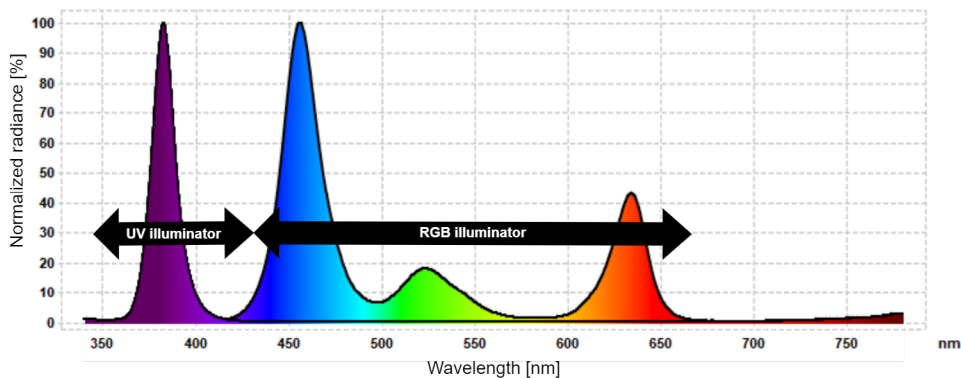


Fig. 5. Spectral characteristics of the illuminators used in the imaging process

a resolution of 2304×2304 pixels and a pixel size of 6.5×6.5 μm was used in the study. The sensor allows the recording of electromagnetic radiation from 300 to 1100 nm (Figure 3). Also, a bandpass filter was used to record electromagnetic radiation in the 300–400 nm range; this restricted imaging to the ultraviolet range. In the remainder of the work, the images recorded using this camera will be referred to as UV images.

The second camera used for imaging was equipped with a Sony IMX 174 sensor in the colour version, enabling image acquisition in the range of electromagnetic radiation from 400 to 1000 nm. The sensor quantum efficiency (QE) plots for each channel are presented in Figure 4. In the remainder of the work, the images recorded using this camera will be referred to as RGB images.

The study concerned the possibility of detecting wood surface defects in the form of fungal infections present on the surface of wood which are invisible to the human eye. A combination of visible light and ultraviolet imaging was used to capture these features (Figure 5). It was expected that this approach would allow the capture of three different images of the same infection. This serves to enhance the different features of the infected area, enabling the assessment of surface defects based on a combination of the recorded images. Figure 5 shows the spectral characteristics of the UV and RGB illuminators.

The spatial resolution of imaging depends on the resolution of the sensor used and, at the same time, on the optical system, i.e. the lens used in the camera. The field of view for both cameras was set so that it is possible to record an image of a wood surface with dimensions of 200×200 mm. The imaging resolution for both cameras was determined based on the dimensions of the field of view and the sensor's resolution expressed in pixels. The UV camera effectively utilises

the 2000×2000 pixel area from the 2304×2304 pixel sensor. The imaging resolution was determined from the following relationships:

$$\Delta X_{UV} = \Delta Y_{UV} = \frac{200[mm]}{2000[pixel]} = 0.1[mm/pixel] \quad (1)$$

This means that a scene area of 0.1×0.1 mm is projected onto one pixel of the UV image. For comparability reasons, the resolution was adjusted to 0.2 mm/pixel.

The RGB camera effectively utilises 1000×1000 pixels from an IMX 174 sensor with a resolution of 1936×1216 pixels. The imaging resolution was determined according to the following relationship:

$$\Delta X_{RGB} = \Delta Y_{RGB} = \frac{200[mm]}{1000[pixel]} = 0.2[mm/pixel] \quad (2)$$

The imaging resolutions for both cameras are the same. The purpose of these settings was to compare the two types of images and simultaneously combine the images to indicate possible differences depending on the spectral range of the imaging. There are 25 pixels in the image for every square millimetre of surface. Exposure time and acquisition time vary, depending on the wood species and the moisture of the wood. Exposure time is selected in the range of a few milliseconds to tens of milliseconds.

Wood surface images were recorded for three types of material used in production. The first type of material was referred to as “fresh” wood, delivered to the plant and sent directly to production. Wood samples were selected during unloading, assuming that such wood is exposed to the development of fungal infections only during sawmill processing or transport to the production plant.

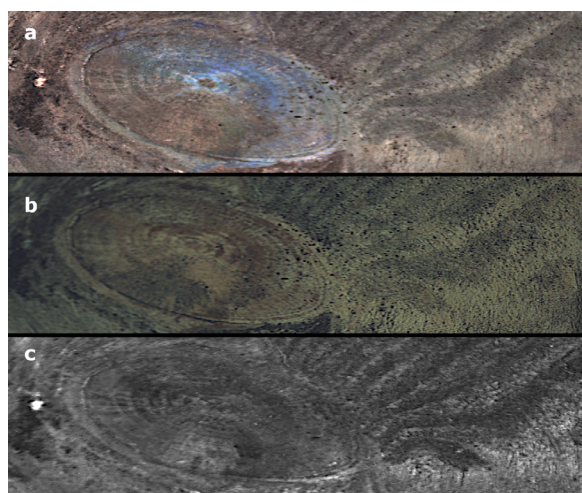


Fig. 6. Examples of wood surface images: a – RGB camera with RGB+UV illumination, b – RGB camera with RGB illumination, c – UV camera with UV illumination

The second type of material was referred to as “stored” wood. The wood was delivered to the plant and stored for several days in the warehouse. At that time, fungal infections were developing on the surface. The dynamics of infection development are very different and depend on the moisture content of the wood and the overall weather conditions, during both transport and storage.

The third type of material was referred to as “dry” wood. Dry wood is wood that has not been exposed to excess moisture during storage and mechanical processing. It has been delivered to the production plant without delays and stored in a well-ventilated place or dried after delivery. In this case, conditions on the surface of the wood did not favour the development of infection.

Three different images were recorded for defect evaluation (Figure 6). The images were recorded with constant image acquisition parameters, but with differences in the way in which the surface was illuminated. Both illuminators were used at the same time, and then each of them separately. Images were registered in the following configurations:

- RGB image recorded in the range 400–1000 nm with the use of an RGB illuminator and a UV illuminator at the same time,
- RGB image recorded in the range 400–1000 nm with the use of only an RGB illuminator,
- UV image recorded in the 300–400 nm range using only a UV illuminator.

Results and discussion

The images were recorded for the three different groups of materials described as fresh wood, stored wood and dry wood (Figure 7). Fungal infections are visible on the surface of fresh wood (Figure 7.1a–c) and stored wood (Figure 7.2a–c). However, the visibility of the infection depends on the camera and light used for acquisition.

Figures 7.1a, 7.1b and 7.1c show images captured with an RGB camera and UV and RGB illuminators operating at 12 W. Images 1a and 1b clearly show the infected areas. These infections are perceptible as coloured areas (Figure 7.1a) or intense blooms (Figure 7.2a). The image of dry wood (Figure 7.3a) presents the most homogeneous distribution of intensity and colour, which indicates a low level of fungal infection on the surface of the imaged wood. Different storage policies produce different conditions for the growth of fungi. Lack of moisture and managed temperature create harsh conditions for the development of fungal infection. Drying the wood and storing it in a well-ventilated space effectively prevents the development of infection. The surface of dry wood without infection is visible in the RGB image as a uniformly coloured surface (Fig. 3a and Fig. 3b). If a fungal infection develops on the surface, this is visible on the RGB image as staining on the wood surface (Fig. 1a, Fig. 2a). This can also be visible on UV images as white areas (Fig. 2c). The colour of the wood infection visible in the RGB images is related to the species of fungi developing on the surface.

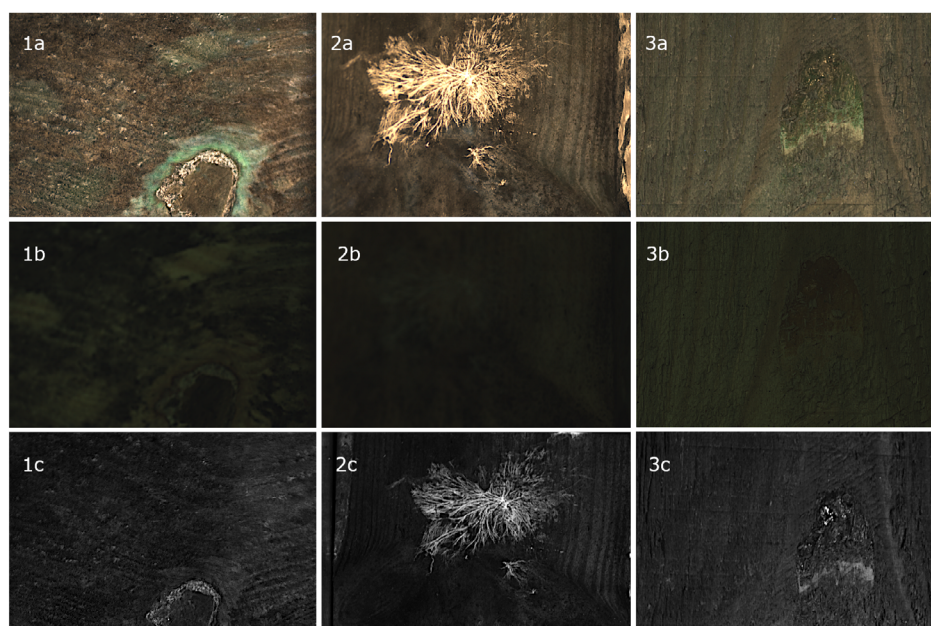


Fig. 7. Sample surface images of wood transported and stored in different conditions:
 1 – fresh wood (green fungi become visible on RGB image under VIS and UV illumination),
 2 – stored wood (white fungi become visible on RGB and UV images under VIS and UV illumination),
 3 – dry wood (as a reference); a – RGB image illuminated by VIS+UV light, b – RGB image illuminated by VIS light,
 c – UV image illuminated by UV light

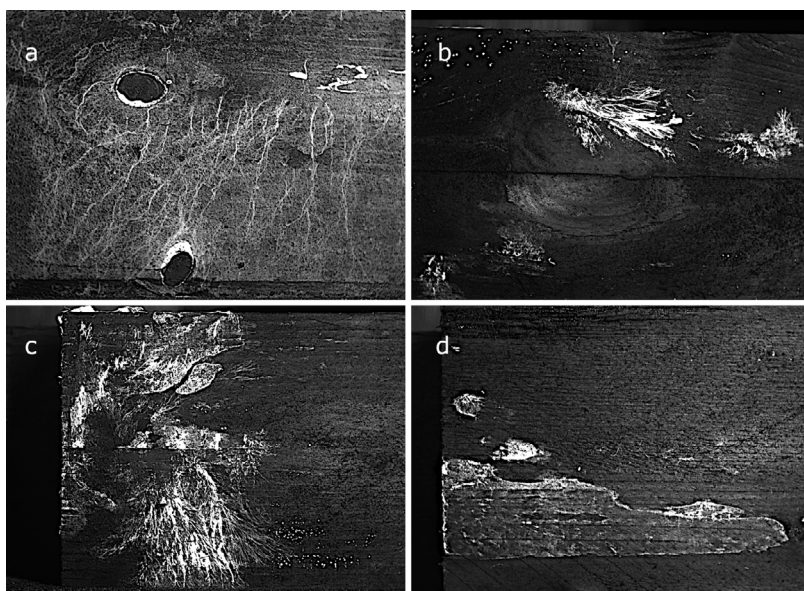


Fig. 8. Examples of UV images of wood surfaces infected with fungi captured with the power of the UV illuminator at 20 W

It is observed that the visibility of infections in RGB images depends on how the surface is illuminated. The simultaneous use of UV and RGB illuminators enhances the infected area on the image. However, turning off the UV illuminator changes the conditions for image capture. Recording the image using only an RGB illuminator makes the traces of infection practically invisible on the surface. These images are shown in Figures 7.1b, 7.2b and 7.3b. It should be noted that these images were recorded using the same camera and the same image acquisition parameters. The low intensity of the images is due to the selection of the image acquisition time and the power of the RGB illuminator used to illuminate the wood surface.

The third series of images (Figures 7.1c, 7.2c, and 7.3c) was recorded using a UV sensor and a UV illuminator. Figures 7.1c and 7.2c show infected areas in the form of areas of increased intensity. The surface of the uninfected wood is visible in these images in the form of a dark background. These images make it possible to observe fungal infections invisible to the human eye. In this case, the key is to select the power of the UV illuminator to increase the intensity of the infected areas.

Subsequent studies involved capturing UV images under illumination power ranging from 5 to 20 W. Based on preliminary tests, a power of 20 W was chosen for imaging due to the possibility of recording relatively high intensities of the infection image (Fig. 8). This allows the infection to be clearly observed against a dark background corresponding to an uninfected wood surface. Selected images acquired using the ORCA camera with a UV illuminator power of 20 W, exhibiting the highest intensity, are presented in Figure 8.

The maximum image acquisition and analysis time was adopted for the planned industrial application to

enable production with the intended efficiency. During this time, the UV and RGB cameras should capture images with high contrast.

With a constant exposure time, increasing the power of the illuminator allows more light to be reflected from the wood surface and recorded on the RGB and UV sensors. Increasing the illuminator power increases the contrast between infected and non-infected areas. The reason for this is the differing absorption of UV light in both areas. In case of the use of insufficient illuminator power and fixed exposure time, the recorded image would have poor contrast and would not allow effective detection of infected areas.

The proposed solution extends imaging possibilities in the visible light range by stimulating infected areas to photoluminescence using UV light.

The acquisition parameters were selected so that the surface of the wood without infection was visible as a homogeneous dark background. The low-intensity areas shown in Figure 8 correspond to a natural surface without infection. The bright areas seen there are infected areas that reflect ultraviolet light. Therefore, it is possible to select imaging parameters so that only infections that have developed on the surface are visible on a dark background.

Based on the results presented in Figures 7.1a and 7.2a, it is also proposed to increase the power of UV and RGB illuminators when recording images using an RGB camera. An increase in power was made to enhance further the features of the infection recorded in the form of a colour image (Figure 9). The image was recorded with UV and RGB illuminators operating at 20 W.

The possibility of observing colours corresponding to fungal infections present on wood results from the

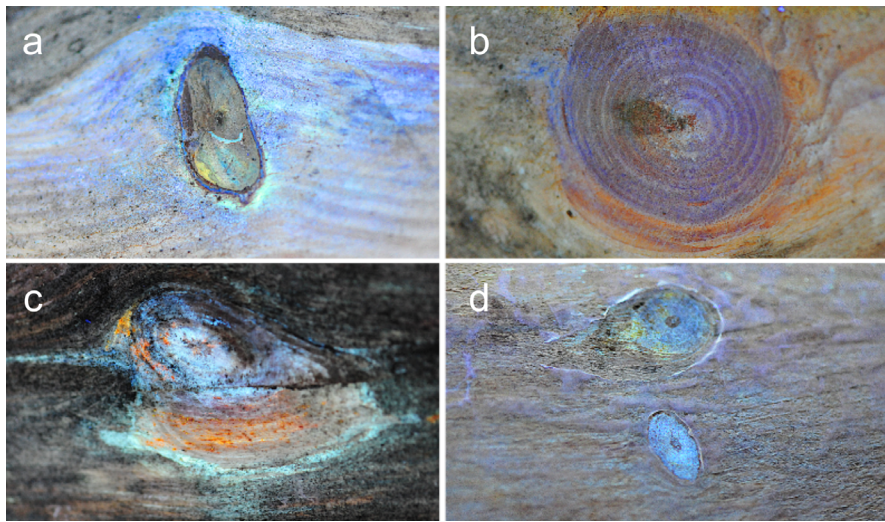


Fig. 9. Sample RGB images of a fungus-infested wood surface captured with a combination of UV and RGB illumination

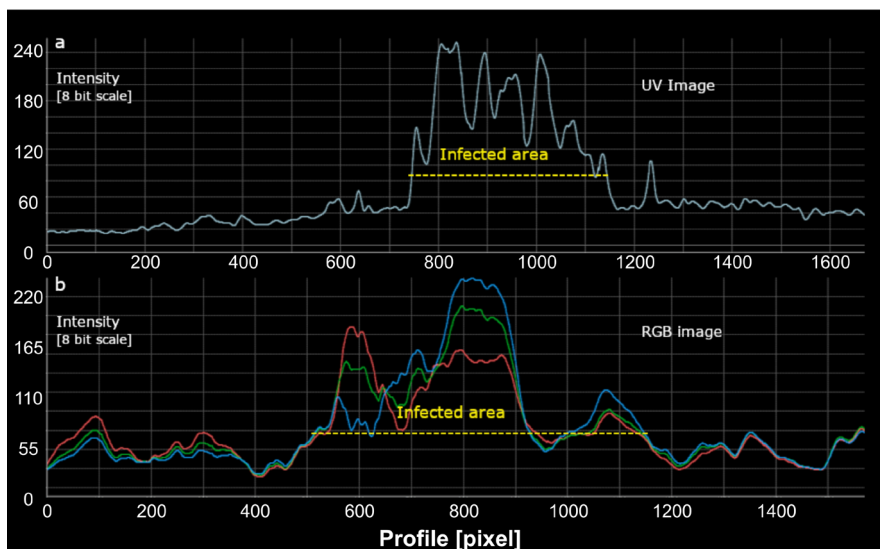


Fig. 10. Intensity profile analysis in the infected areas: a – profile from UV image, b – profile from RGB image

phenomenon of photoluminescence, activated by a UV light of precise wavelength. The energy delivered to infected surfaces from the UV illuminator is absorbed by specific particles of fungi. The absorbed photons of light cause the electrons to move to higher energy states. During the return transition to lower energy states, energy is released through the emission of photons of particle-dependent wavelength. Capturing the RGB image in the visible range allows the recording of this radiation, which causes the infected areas to be “coloured”.

The interaction of light with fungal infections varies depending on the fungal species. Some such species reflect UV light, allowing observation of infection in the ultraviolet range. Other species absorb UV light, making the infections invisible in UV images. The energy absorbed by fungal infections may activate light emission in the visible light range. This re-emission

is manifested by the colour patterns generated by the various fungal species seen in visible light.

Both UV and UV+RGB imaging confirmed that the high moisture content of wood and the lack of ventilation of the material results in rapid growth of the infection. Images recorded on fresh and stored wood in conditions of high humidity show an increase in the visibility of fungal infections in the ultraviolet range.

Analysis of the intensity of the sample profile performed on the UV and RGB images indicates that the infected areas are well identifiable against the background of the non-infected areas (Figure 10). In the UV image shown in Figure 10a, the infected area has an intensity several times higher than that of areas where infections have not developed. The intensity of the areas without infection ranges from 0 to 60, expressed on an 8-bit scale. Infected areas, on the other hand, are

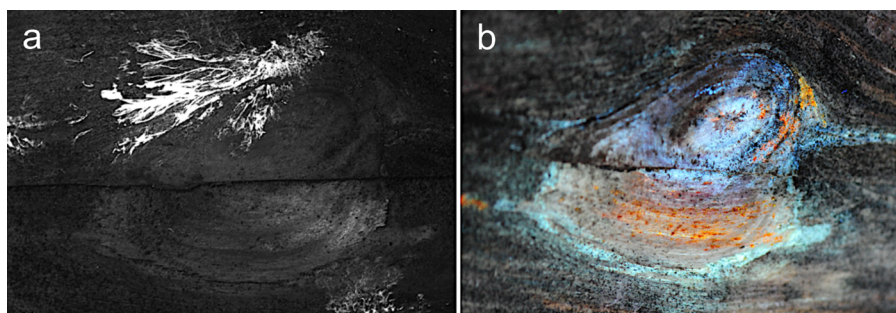


Fig. 11. Images of infected wood: a – UV image, b – RGB image

described with values from 60 to 240. The RGB image also shows a significant increase in intensity in each channel relative to the uninfected surface (Figure 10b). Therefore, the images recorded in this way provide information that can be used to identify the presence of fungal infections on the surface of the wood.

The study had the aim of developing a system for rapid imaging of infections on the surface of wood. However, the recorded images can be used not only to identify the presence of infection on wood. The analysis of colours in RGB images and the intensity of infected areas in UV images may be used in the future to identify the species of fungi growing on the surface of wood. The picture below shows two images of the same wood surface with a visible knot. Both images show areas where infections have developed. It should be noted that the image recorded in UV shows a different infection than the image recorded in visible light. The fungus shown in Figure 11a is not recorded in the RGB image.

The proposed solution takes the form of a laboratory stand for the innovative imaging of wood surfaces to detect fungal infections. The construction of a prototype of an industrial version needs to consider the maintenance of constant lighting conditions. It requires the development of an enclosure and limiting of the impact of external light, including natural and artificial lighting. This will enable stable operation of the imaging system regardless of the time of day, season, and weather.

Another potential interference source is dust and dirt in industrial environments. This requires developing a system to protect the lenses and illuminators, as well as cleaning systems for the imaging workspace.

Conclusions

The solution presented in this paper was created as a response to a specific need of a production plant using wood in the production process. The designed system of illuminators and sensors allows the observation of various types of infection visible in both UV images and images recorded in the visible light range. This type of imaging requires the use of more powerful illuminators. Adjustable illuminators with a maximum

power of 20 W were used in the study. The proposed imaging method makes it possible to compare the two results and identify more infections occurring together on a single surface. There is an explicit dependence of the features of the infected area visible in the image on the type of infection, the spectral range of imaging, and the spectral characteristics of the illuminators used.

A significant limitation is the system acquisition time. In the case of efficient industrial production, camera scan area and illuminator switching frequency may need to be higher. Further work will be carried out with the aim of designing an industrial-scale prototype. Linear cameras and linear illuminators will be included in the research. Their use would allow flow-mode operation and a reduction in image acquisition time. Work is also being carried out on surface evaluation algorithms. With the wood surface depicted in RGB images with VIS illumination, RGB images with VIS+UV illumination, and UV images with UV illumination, the challenge remains to develop high-performance image analysis algorithms. Given the amount of data, ML and AI methods will be considered alongside classical image analysis algorithms.

The proposed imaging system allows the recording of images of infection in laboratory and industrial conditions. Images obtained by this method can be used to identify infections present in wood. Further work will be carried out to enable identification of the species of fungi infesting the wood based on the analysis of both recorded images.

Obstacles to industrial application include sources of interference encountered on production lines, the efficiency of the system, and the need to develop image processing algorithms to ensure correct and reliable automation of the quality control task.

Another possible direction of development is the classification of detected fungi into species based on analysis of the light spectrum emitted by photoluminescence. Information about a fungal species may be linked to the specific conditions of its occurrence. Knowledge about the occurrence of fungal species enables the adaptation of storage and transport processes. Such information could be used to reduce the use of wood preservative treatments by focusing on the elimination of specific fungal species.

References

- Bucur, V. (2003).** Techniques for high resolution imaging of wood structure: a review. *Measurement Science and Technology*, 14(12), R91–R98. <https://doi.org/10.1088/0957-0233/14/12/R01>
- Chun, T. H., Hashim, U. R. A., Ahmad, S., Salahuddin, L., Choon, N. H., & Kanchymalay, K. (2023).** A review of the automated timber defect identification approach. *International Journal of Electrical & Computer Engineering*, 13(2), 2088–8708. <https://doi.org/10.11591/ijece.v13i2.pp2156-2166>
- Cinal, M., Sioma, A., & Lentz, B. (2023).** The Quality Control System of Planks Using Machine Vision. *Applied Sciences (Switzerland)*, 13(16). <https://doi.org/10.3390/app13169187>
- Du, W., Xi, Y., Harada, K., Zhang, Y., Nagashima, K., & Qiao, Z. (2021).** Improved Hough Transform and Total Variation Algorithms for Features Extraction of Wood. *Forests*, 12(4), 466. <https://doi.org/10.3390/f12040466>
- Funck, J. W., Zhong, Y., Butler, D. A., Brunner, C. C., & Forrer, J. B. (2003).** Image segmentation algorithms applied to wood defect detection. *Computers and Electronics in Agriculture*, 41(1–3), 157–179. [https://doi.org/10.1016/S0168-1699\(03\)00049-8](https://doi.org/10.1016/S0168-1699(03)00049-8)
- Haciefendioglu, K., Bařaga, H. B., Bulut, M. C., & Kartal, M. E. (2022).** Automatic Damage Detection on Traditional Wooden Structures with Deep Learning-Based Image Classification Method. *Drvna Industrija*, 73(2), 163–176. <https://doi.org/10.5552/drvid.2022.2108>
- He, T., Liu, Y., Yu, Y., Zhao, Q., & Hu, Z. (2020).** Application of deep convolutional neural network on feature extraction and detection of wood defects. *Measurement*, 152, 107357. <https://doi.org/10.1016/j.measurement.2019.107357>
- Hu, C., Tanaka, C., & Ohtani, T. (2004a).** Locating and identifying sound knots and dead knots on sugi by the rule-based color vision system. *Journal of Wood Science*, 50(2), 115–122. <https://doi.org/10.1007/s10086-003-0549-3>
- Hu, J., Yu, X., Zhao, Y., Wanh, K., & Lu, W. (2022b).** RESEARCH ON BAMBOO DEFECT SEGMENTATION AND CLASSIFICATION BASED ON IMPROVED U-NET NETWORK. *Wood Research*, 67(1), 109–122. <https://doi.org/10.37763/wr.1336-4561/67.1.109122>
- Jankowiak, R. (2013).** Assessing the virulence of ophiostomatoid fungi associated with the pine-infesting weevils to scots pine *Pinus sylvestris* L. seedlings. *Acta Agrobotanica*, 66(2), 85–94. <https://doi.org/10.5586/aa.2013.026>
- Kamiński, A. (2018).** „Inteligentna fabryka” – nowe trendy w rozwoju systemów informatycznych dla przemysłu, Zarządzanie i Finanse, *Journal of Management and Finance*, 16(3), 113–122. http://www.wzr.ug.edu.pl/.zif/11_9.pdf
- Kammerbauer, R., Schmitt, T. H., & Bocklet, T. (2024).** Segmenting Wood Rot using Computer Vision Models. *arXiv preprint*, arXiv:2409.20137. <https://doi.org/10.48550/arXiv.2409.20137>
- Kubicek, C. P., Steindorff, A. S., Chenthamara, K., Manganiello, G., Henrissat, B., Zhang, J., Cai, F., Kopchinskiy, A. G., Kubicek, E. M., Kuo, A., Baroncelli, R., Sarrocco, S., Noronha, E. F., Vannacci, G., Shen, Q., Grigoriev, I. V., & Druzhinina, I. S. (2019).** Evolution and comparative genomics of the most common Trichoderma species. *BMC Genomics*, 20(1), 485. <https://doi.org/10.1186/s12864-019-5680-7>
- Lentz, B. (2020).** Tree-ring growth measurements automation using machine vision. In R. S. Romaniuk & M. Linczuk (Eds.), *Photonics Applications in Astronomy, Communications, Industry, and High Energy Physics Experiments 2020* (Issue October, p. 30). SPIE. <https://doi.org/10.1117/12.2580513>
- Lentz, B., & Kwiek, P. J. (2021).** Quality control automation of metallic surface using machine vision. In A. Smolarz, R. S. Romaniuk, & W. Wojcik (Eds.), *Photonics Applications in Astronomy, Communications, Industry, and High Energy Physics Experiments 2021* (Vol. 2021, Issue November 2021, p. 28). SPIE. <https://doi.org/10.1117/12.2613807>
- Lin, L., He, S., Fu, F., & Wang, X. (2015).** Detection of wood failure by image processing method: influence of algorithm, adhesive and wood species. *European Journal of Wood and Wood Products*, 73(4), 485–491. <https://doi.org/10.1007/s00107-015-0907-z>
- Linnakoski, R., de Beer, Z. W., Ahtiainen, J., Sidorov, E., Niemelä, P., Pappinen, A., & Wingfield, M. J. (2010).** *Ophiostoma* spp. associated with pine- and spruce-infesting bark beetles in Finland and Russia. *Persoonia – Molecular Phylogeny and Evolution of Fungi*, 25(1), 72–93. <https://doi.org/10.3767/003158510X550845>
- Meinlschmidt, P. (2005).** Thermographic detection of defects in wood and wood based materials. *14th International Symposium of Nondestructive Testing of Wood, Germany (May 2nd-4th 2005)*, 269206, 6. <https://www.ndt.net/article/v11n01/meinlschmidt/meinlschmidt.pdf>
- Ondrejka, V., Gergeľ, T., Bucha, T., & Pástor, M. (2021).** Innovative methods of non-destructive evaluation of log quality. *Central European Forestry Journal*, 67(1), 3–13. <https://doi.org/10.2478/forj-2020-0021>
- Romano, E., Brambilla, M., Bisaglia, C., Assirelli, A. (2023)** Using Image Texture Analysis to Evaluate Soil-Compost Mechanical Mixing in Organic Farms. *Agriculture*, 13(6), 1113. <https://doi.org/10.3390/agriculture13061113>
- Sioma, A. (2015).** Assessment of wood surface defects based on 3D image analysis. *Wood Research*, 60(3), 339–350. <https://www.woodresearch.sk/wr/201503/01.pdf>
- Sioma, A. (2019a).** 3D imaging methods in quality inspection systems. In R. S. Romaniuk & M. Linczuk (Eds.), *Photonics Applications in Astronomy, Communications, Industry, and High-Energy Physics Experiments*

- 2019 (Issue November, p. 91). SPIE. <https://doi.org/10.1117/12.2536742>
- Sioma, A. (2019b).** Quality control system of wooden flanges based on vision measurement system. *Wood Research*, 64(4), 637–646.
- Sioma, A. (2020).** Geometry and resolution in triangulation vision systems. In R. S. Romaniuk & M. Linczuk (Eds.), *Photonics Applications in Astronomy, Communications, Industry, and High Energy Physics Experiments 2020* (Issue October, p. 33). SPIE. <https://doi.org/10.1117/12.2580525>
- Sioma, A., Socha, J., & Klamerus-Iwan, A. (2018).** A New Method for Characterizing Bark Microrelief Using 3D Vision Systems. *Forests*, 9(1), 30. <https://doi.org/10.3390/f9010030>
- Wakaf, Z., & Jalab, H. A. (2018).** Defect detection based on extreme edge of defective region histogram. *Journal of King Saud University – Computer and Information Sciences*, 30(1), 33–40. <https://doi.org/10.1016/j.jksuci.2016.11.001>
- Wei, Q., Chui, Y. H., Leblon, B., & Zhang, S. Y. (2009).** Identification of selected internal wood characteristics in computed tomography images of black spruce: a comparison study. *Journal of Wood Science*, 55(3), 175–180. <https://doi.org/10.1007/s10086-008-1013-1>
- Wells, L., Gazo, R., Re, R. D., Krs, V., & Benes, B. (2018).** Defect detection performance of automated hardwood lumber grading system. *Computers and Electronics in Agriculture*, 155, 487–495. <https://doi.org/10.1016/j.compag.2018.09.025>
- Yi, L. P., Akbar, M. F., Wahab, M. N. A., Rosdi, B. A., Fauthan, M. A., & Shrifan, N. H. M. M. (2024).** The Prospect of Artificial Intelligence-Based Wood Surface Inspection: A Review. *IEEE Access*, 12, 84706–84725. <https://doi.org/10.1109/ACCESS.2024.3412928>